Suspended SOI waveguide with sub-wavelength grating cladding for mid-infrared

J. Soler Penadés,[1,*] C. Alonso-Ramos,[2] A. Z. Khokhar,[1] M. Nedeljkovic,[1] L. A. Boodhoo,[3] A. Ortega-Moñux,[2] I. Molina-Fernández,[2] P. Cheben,[4] and G. Z. Mashanovich[1]

[1] *Optoelectronics Research Centre, University of Southampton, Southampton SO17 1BJ, United Kingdom*

[2] *Departamento de Ingeniería de Comunicaciones , Universidad de Málaga, 29071 Málaga, Spain*

[3] *Electronics and Computer Science, University of Southampton, Southampton SO17 1BJ, United Kingdom*

[4] *National Research Council Canada, Building M-50, Ottawa, K1A 0R6 Canada*

compiled: August 13, 2014

We present a new type of mid-infrared silicon-on-insulator (SOI) waveguide. The waveguide comprises a sub-wavelength lattice of holes acting as lateral cladding while at the same time allowing for the bottom oxide (BOX) removal by etching. The waveguide loss is determined at the wavelength of 3.8 μm for structures before and after being underetched using both vapour phase and liquid hydrofluoric acid (HF). A propagation loss of 3.4 dB/cm was measured for a design with a 300nm grating period and 150nm holes after partial removal (560nm) of BOX by vapour phase HF etching. We also demonstrate an alternative design with 550nm period and 450nm holes, which allows a faster and complete removal of the BOX by liquid phase HF etching, yielding the waveguide propagation loss of 3.6 dB/cm.

OCIS codes: (130.0250) Optoelectronics; (130.3060) Infrared; (130.3120) Integrated optics devices; (230.7390) Waveguides, planar.

http://dx.doi.org/10.1364/XX.99.099999

SOI has become the most dominant platform for building integrated silicon photonic devices at telecom wavelengths in near-infrared. However the increasing absorption loss of SiO_2 at longer wavelengths makes it challenging to utilize SOI for low-loss components in the mid-infrared (MIR) [1]. Removing the SiO_2 layer opens the possibility of extending the low-loss SOI wavelength range up to ~8μm, benefiting from the established fabrication techniques and high quality SOI material [2, 3]. SiO_2 removal can be accomplished by using periodic holes formed on the side of the waveguide core. A minimum waveguide propagation loss of 3.0±0.7dB/cm at 2.75μm was reported for this approach in [4], but the fabrication involved 2 dry etch steps, one to define the rib waveguide and another to etch the holes which are subsequently used for the SiO_2 removal by HF etching.

In this paper we introduce a new concept for making SOI waveguides for the MIR. The concept is based on forming a sub-wavelength lattice of holes acting as the lateral waveguide cladding while, at the same time, allowing the BOX removal by HF etching. A practical advantage of this technique is that only 1 dry etch step is required. Furthermore, the structure mechanical stability is improved given that the suspended waveguide is comparatively thicker since there rib waveguide remains un-etched, unlike in [4].

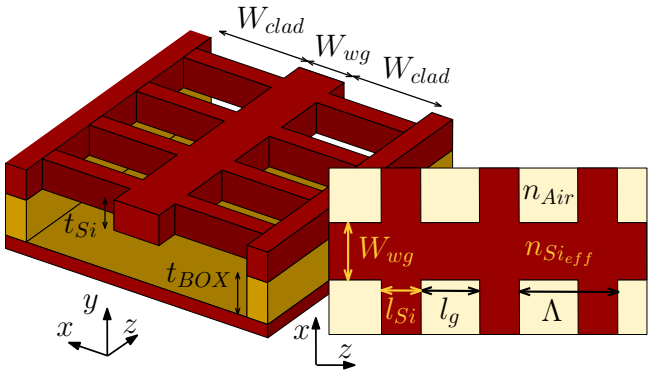

Fig. 1. Schematic representation of the suspended waveguide with sub-wavelength grating lateral cladding.

The waveguide core and the sub-wavelength cladding are designed using Bloch-Floquet mode calculations with a Fourier Eigenmode Expansion Method (F-EEM) simulator [5]. The effective Index Method (EIM) is applied to obtain a simplified 2D structure (see inset in Fig. 1). For waveguide and BOX thicknesses of t_{Si}=500 nm and t_{BOX}=3 μm, respectively, and assuming air as the bottom and upper medium, the effective index for the silicon slab waveguide at 3.8 μm wavelength and TE (in-plane)

* Corresponding author: jsp1g12@soton.ac.uk

polarization is $n_{Si_{eff}}$=2.67.

Waveguide width is set to $W_{wg} = 1.1\,\mu$m to ensure single-mode behaviour. In order to suppress diffraction effects in the sub-wavelength cladding region and reduce back-reflections, it is required that the grating period (Λ) is shorter than the Bragg period (Λ_B) [6, 7].

$$\Lambda = l_{Si} + l_g < \Lambda_B = \frac{\lambda_0}{2n_{BF}} \tag{1}$$

where l_{Si}, l_g are the silicon strip and gap lengths in the sub-wavelength cladding, respectively (see Fig. 1), and n_{BF} is the effective index of the fundamental Bloch-Floquet mode propagating in the waveguide. On the other hand, a larger gap size is beneficial to facilitate liquid HF penetration for BOX removal. Within the sub-wavelength regime, the ratio of l_g and l_{Si} determines the equivalent index synthesized by the structure [8]. With an increasing ratio l_g/l_{Si}, the equivalent cladding refractive index decreases, yielding an increase in the waveguide index contrast and modal confinement. It is well established in the field that the waveguide propagation losses increase with the index contrast, but the study of this effect for our specific waveguide geometry is beyond the scope of this paper.

Figure 2 shows calculated back-reflections as a function of the gap length for silicon strip lengths of 100 nm, 150 nm and 200 nm, ensuring structure's mechanical stability. The simulations show that the maximum allowable gap length to suppress Bragg effect and resulting back-reflections increases for thinner l_{Si}. Sub-wavelength cladding width (W_{clad}) is designed to avoid light leakage to the lateral silicon region. Bloch-Floquet mode field distribution is represented in the inset of Fig. 2 for two different sub-wavelength cladding configurations. It is observed that the modes exhibit an intensity decay exceeding 40 dB at points $\pm 4\,\mu$m away from the waveguide center. Therefore, we conclude that cladding width $W_{clad} = 5\,\mu$m is large enough to ensure negligible lateral leakage.

The waveguides were written using a JEOL JBX 9300FS e-beam lithography tool on 6-inch SOI wafers with 3μm BOX and 500nm Si overlayer. ZEP-520A was used as a positive resist. Patterns in ZEP-520A were transferred to the SOI wafers by inductively coupled plasma (ICP) using an Oxford Instruments ICP 380 plasma system.

The dimensions of the first waveguide design were W_{wg}=1.1 μm, W_{clad}=4 μm. Sub-wavelength cladding dimensions were set to l_{Si}=150 nm, l_g=150 nm, to avoid Bragg reflections and to provide both sufficient mechanical stability and holes large enough to allow vapour HF penetration for BOX removal. The wafer was then dry etched to a depth of 500 nm. The BOX was further etched by 560 nm using vapour phase HF in an Idonus HF vapour phase etcher tool. The latter was used since it was confirmed experimentally that this gap size was too small ($l_g = 150$ nm) to allow etching with liquid HF. The vapour phase process was found to be very slow, due

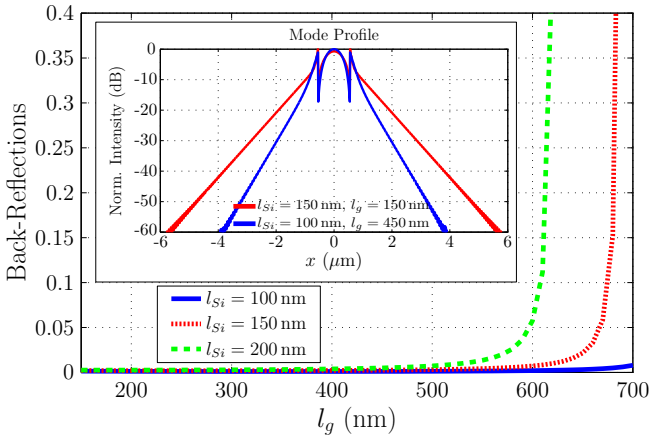

Fig. 2. Calculated back-reflections as a function of sub-wavelength cladding gap length (l_g) for silicon strip lengths (l_{Si}) of 100 nm, 150 nm and 200 nm. Inset shows Bloch-Floquet mode field distribution for l_{Si} = 150 nm and l_{Si} = 100 nm, with l_g = 150 nm and l_g = 450 nm respectively.

to the build-up of water as the reaction by-product. The etch rate was initially ~30 nm per minute but dropped to close to zero after 3.5 minutes of etching. The sample was subsequently dehydrated in an oven at 220 °C for 10min and left to cool down for 3min as the optimum temperature for etching was 40 °C.

We used focussing surface grating couplers for the input and output coupling, to circumvent difficulties with cleaving consistently the under-etched waveguides. Surface grating efficiency was optimized by sub-wavelength refractive index engineering [9], the concept originally proposed by Halir et al. [10, 11]. Half of the waveguides in the design also included a taper between the grating and the waveguide (fig. 3), because the focal field size from the grating was expected to be slightly larger compared to the waveguide mode size. The other half of the design had the same waveguide dimensions but no tapers between input/output claddings and the waveguide.

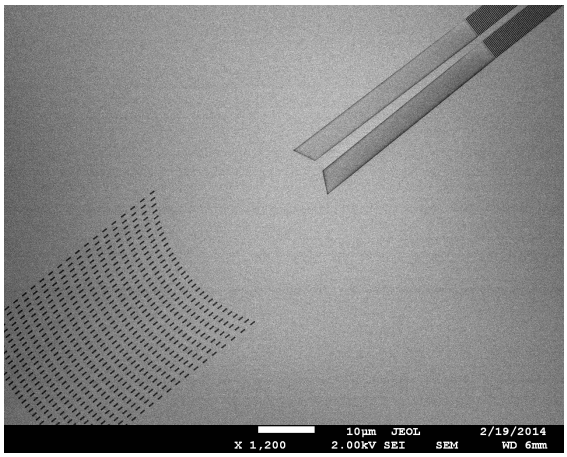

Fig. 3. SEM image of the waveguide with SWG cladding, focussing coupling grating and taper.

The cut back method was used to determine the waveguide propagation loss. We measured the transmission at 3.8 μm wavelength through straight waveguides with lengths between 0.6 cm and 2.35 cm using the experimental setup described in [12]. The propagation loss before vapour phase HF etching was 4.7 dB/cm, and it was reduced to 3.4 dB/cm after etching to a depth of approximately 560 nm. The waveguide loss measurement results are shown in figure 4. We attribute this loss reduction to the partial removal of the SiO_2 BOX and better vertical confinement of the mode within the core of the waveguide. The waveguides with and without tapers were found to have identical loss. Therefore, since the long strip of silicon unsupported in the taper could introduce undesired mechanical instability to the interface between the grating and the waveguide, the tapers were not included in our further designs.

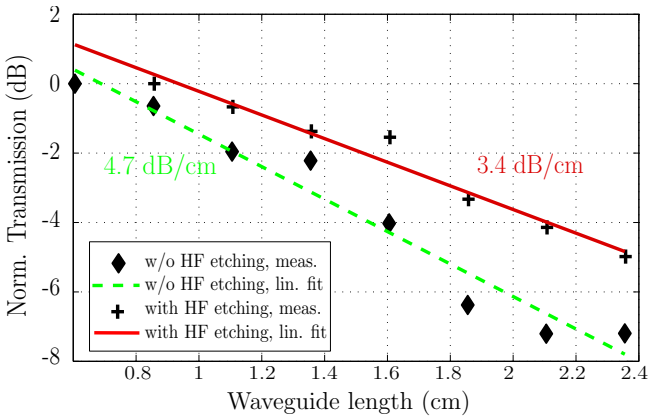

Fig. 4. Subwavelength waveguide loss measurement before and after HF vapour phase etching. The transmission measurements are normalized to the transmission of the shortest waveguide in the respective section. The green (dashed) line is a linear fit to measured data (diamond symbols) before vapour phase HF etching (loss 4.7dB/cm). The red line is a linear fit of the measured data (cross symbols) after HF etching (loss 3.4dB/cm).

In the subsequent experiment, a new set of waveguides was fabricated with the same dimensions as the previous design except for l_{Si}=100 nm and l_g=450 nm, i.e. with a larger gap and smaller silicon strip. This allowed etching the BOX with liquid HF, substantially shortening etch time. Also, according to simulations (fig. 2), larger l_g would provide better mode containment in the core of the waveguide with smaller l_{Si} fulfilling the requirement to suppress the Bragg effect. The chips were then immersed for 30 minutes in a 1:7 HF solution, yielding an etch depth of approximately 2.5 μm. The fabricated waveguide is shown in figure 5.

The waveguide propagation loss measured before and after 30min HF etching was 5 dB/cm and 3.6 dB/cm. The chips were then immersed for 10 additional minutes in liquid HF, removing the BOX completely. This additional etch damaged a few waveguides as the suspended

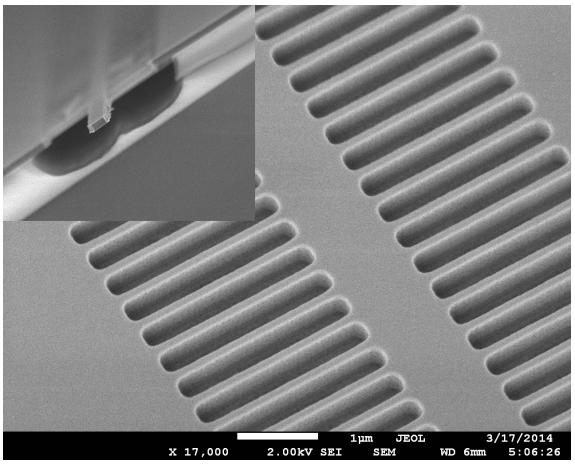

Fig. 5. Top view SEM image of the sub-wavelength grating waveguide after immersion in 1:7 liquid HF for 30 minutes. In the top left inset a SEM image of the facet of a cleaved waveguide, an isotropic etching of the oxide can be observed from the points of entry of the etchant solution. Some of the structural damage to the waveguide produced during cleaving can be also appreciated.

structure width was increased to over 17 μm, but no excess loss penalty was found in those waveguides which remained undamaged. The waveguide loss measurements are shown in figure 6.

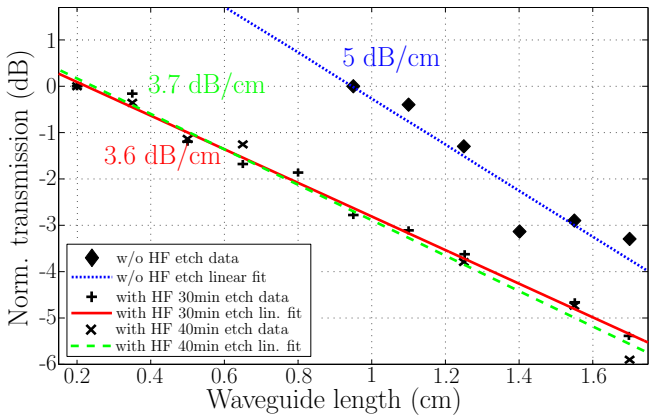

Fig. 6. Subwavelength waveguide loss measurement before and after HF liquid phase etching. The blue (dotted) line: linear fit to measured data (diamond symbols) for the structure with sub-wavelength period 550 nm and 450 nm gaps before etching (loss of 5 dB/cm). The red line: is a linear fit to measured data (cross symbols) after 30min HF etching (loss of 3.6 dB/cm). The green (dashed) line: a linear fit to measured data (ex symbols) after 40min HF etching (loss of 3.7 dB/cm)

In conclusion, in this paper we demonstrated, for the first time, a Si waveguide with sub-wavelength lateral cladding design operating in MIR. Two specific structures were studied, namely Si waveguides with 150 nm cladding holes and 300 nm period under-etched

with vapour phase HF, and Si waveguides with 450 nm cladding holes and 550 nm period etched with liquid HF. The measured propagation losses for the first type was 4.7 dB/cm before under-etching and 3.4 dB/cm afterwards. For the latter type the propagation loss was measured as 5 dB/cm before and 3.6 dB/cm after etching for 30 minutes in a 1:7 HF solution. There was no appreciable difference in the transmission loss when the BOX was completely removed from these chips.

Our sub-wavelength grating MIR waveguide opens the possibility of using a SOI substrate throughout the full MIR transparency range of Si, up to $\sim 8\mu$m, with an additional advantage of using a single etch step fabrication. Unlike in previously reported structures [4, 13] the lateral holes in our design are an integral part of the waveguide cladding and serve a double purpose, i.e. for optical confinement and as etch access points. Such structure can also provide efficient mode field overlap with a surrounding fluid or gas. These advantages, along with the increased operational wavelength range, make this type of waveguide a promising candidate for gas sensing application. We expect the propagation loss could be further reduced with fabrication process optimization and possibly with surface smoothing by thermal oxidation. The fabrication requirements would also be more relaxed at longer wavelengths given the comparatively larger hole size. This new type of MIR Si waveguide opens excellent prospects for using a SOI substrate over the full MIR transparency range of silicon.

Acknowledgements

The authors are grateful to Xia Chen for the design of grating couplers. G. Z. Mashanovich acknowledges support from the Royal Society through his fellowship. A part of this work was funded by the EPSRC project MIGRATION.

References

[1] M. Nedeljkovic, A. Khokhar, Y. Hu, X. Chen, J. Penades, S. Stankovic, H. Chong, D. Thomson, F. Gardes, G. Reed, and G. Mashanovich, "Silicon photonic devices and platforms for the mid-infrared," Opt. Mater. Express 3, 1205-1214 (2013).

[2] R. A. Soref, S. J. Emelett, W. R. Buchwald, "Silicon waveguided components for the long-wave infrared region," J. Opt. A 8, 840-848 (2006).

[3] R. Soref, "Mid-infrared photonics in silicon and germanium," Nature Photonics 4, 495-497 (2010).

[4] Cheng, Z., Chen, X., Wong, C. Y., Xu, K., Tsang, H. K., "Mid-infrared suspended membrane waveguide and ring resonator on silicon-on-insulator," Photonics Journal, IEEE , 4, no.5, 1510-1519 (2012).

[5] L. Zavargo-Peche, A. Ortega-Moñux, J.G. Wangüemert-Pérez, and I. Molina-Fernández, "Fourier based combined techniques to design novel sub-wavelength optical integrated devices," Prog. Electromagn. Res., 123, 447 (2012).

[6] P. J. Bock, P. Cheben, J. H. Schmid, J. Lapointe, A. Delâge, S. Janz, G. C. Aers, D.-X. Xu, A. Densmore, and T. J. Hall, "Subwavelength grating periodic structures in silicon-on-insulator: a new type of microphotonic waveguide," Opt. Express, 18, 20251 (2010).

[7] A. Ortega-Moñux, L. Zavargo-Peche, A. Maese-Novo, I. Molina-Fernández, R. Halir, J. G. Wangüemert-Pérez, P. Cheben, and J. H. Schmid, "High-performance multimode interference coupler in silicon waveguides with subwavelength structures," IEEE Photonics Technol. Lett., 23, 1406 (2011).

[8] S. M. Rytov, "The electromagnetic properties of finely layered medium," Sov. Phys. JETP, vol. 2, p. 466, (1956).

[9] P. Cheben, P. Bock, J. Schmid, J. Lapointe, S. Janz, D. Xu, A. Densmore, A. Delge, B. Lamontagne, and T. Hall, "Refractive index engineering with subwavelength gratings for efficient microphotonic couplers and planar waveguide multiplexers," Opt. Lett. 35, 2526-2528 (2010).

[10] R. Halir, P. Cheben, S. Janz, D. Xu, . Molina-Fernndez, and J. Wangemert-Prez, "Waveguide grating coupler with subwavelength microstructures," Opt. Lett. 34, 1408-1410 (2009).

[11] R. Halir, P. Cheben, J. Schmid, R. Ma, D. Bedard, S. Janz, D. Xu, A. Densmore, J. Lapointe, and . Molina-Fernndez, "Continuously apodized fiber-to-chip surface grating coupler with refractive index engineered subwavelength structure," Opt. Lett. 35, 3243-3245 (2010).

[12] M. Nedeljkovic, "Silicon photonic modulators for the mid-infrared," University of Southampton, Physical Sciences and Engineering, Doctoral Thesis (2013).

[13] Y. Xia, C. Qiu, X. Zhang, W. Gao, J. Shu, and Q. Xu, "Suspended Si ring resonator for mid-IR application," Opt. Lett. 38, 1122-1124 (2013).